



# A unique approach to monitor stress in coral exposed to emerging pollutants

Didier Stien,  Marcelino Suzuki, Alice M. S. Rodrigues, Marion Yvin, Fanny Clergeaud, Evane Thorel, and Philippe Lebaron

Sorbonne Université, CNRS, Laboratoire de Biodiversité et Biotechnologies Microbiennes, USR3579, Observatoire Océanologique, 66650 Banyuls-sur-mer, France

Didier Stien, Email: [didier.stien@cnrs.fr](mailto:didier.stien@cnrs.fr).

 Corresponding author.

Received 2019 Jul 31; Accepted 2020 Apr 15.

Copyright © The Author(s) 2020

**Open Access** This article is licensed under a Creative Commons Attribution 4.0 International License, which permits use, sharing, adaptation, distribution and reproduction in any medium or format, as long as you give appropriate credit to the original author(s) and the source, provide a link to the Creative Commons license, and indicate if changes were made. The images or other third party material in this article are included in the article's Creative Commons license, unless indicated otherwise in a credit line to the material. If material is not included in the article's Creative Commons license and your intended use is not permitted by statutory regulation or exceeds the permitted use, you will need to obtain permission directly from the copyright holder. To view a copy of this license, visit

<http://creativecommons.org/licenses/by/4.0/>.

## Abstract

Metabolomic profiling of the hexacoral *Pocillopora damicornis* exposed to solar filters revealed a metabolomic signature of stress in this coral. It was demonstrated that the concentration of the known steroid (3 $\beta$ , 5 $\alpha$ , 8 $\alpha$ ) -5, 8-epidioxy- ergosta- 6, 24(28) - dien- 3- ol (**14**) increased in response to octocrylene (OC) and ethylhexyl salicylate (ES) at 50  $\mu$ g/L. Based on the overall coral response, we hypothesize that steroid **14** mediates coral response to stress. OC also specifically altered mitochondrial function at this concentration and above, while ES triggered a stress/inflammatory response at 300  $\mu$ g/L and above as witnessed by the significant increases in the concentrations of polyunsaturated fatty acids, lysophosphatidylcholines and lysophosphatidylethanolamines. Benzophenone-3 increased the concentration of compound **14** at 2 mg/L, while the concentration of stress marker remained unchanged upon exposition to the other solar filters tested. Also, our results seemed to refute earlier suggestions that platelet-activating factor is involved in the coral inflammatory response.

**Subject terms:** Environmental impact, Analytical chemistry, Bioanalytical chemistry

## Introduction

Coral reefs are experiencing an unprecedented planet-wide decline<sup>1</sup>. This decline has been attributed to several anthropogenic factors, including global warming, overfishing, and pollution. Widely used for skin protection against cancer, solar filters are regularly released in the sea from populated coastal zones or in sites dedicated to touristic activities including a bathing zone. Nonetheless, the impacts of solar filters on corals have been relatively understudied to date. An early article from Danovaro and coworkers<sup>2</sup> demonstrated that solar filters can induce coral bleaching by promoting viral infections. More recently, it was shown that several UV filters in the benzophenone class, along with octocrylene (OC), exert direct detrimental effects on corals<sup>3,7</sup>. Additionally, it has been shown that other ingredients in sunscreens and cosmetics exacerbate the toxicity of the UV filters OC and octinoxate<sup>8</sup>, while Fel *et al.* reported that many UV filters, including OC have little or no effect on corals<sup>9</sup>.

According to Downs *et al.*, benzophenone-3 (BP3) induced concentration-dependent planulae coral bleaching, DNA-AP lesions, ossification of the planula, and planulae mortality, and these adverse effects were exacerbated by light<sup>3</sup>. In our previous work, we compared the metabolomic profiles of exposed and unexposed corals and demonstrated that OC triggers mitochondrial dysfunction that results in the accumulation of acylcarnitines<sup>7</sup>. Also of great concern were both the accumulation of OC derivatives in coral tissues and the concentration at which the toxicity was detected. In a 1-week exposure experiment, 19 OC derivatives were found in the coral tissue, and the response-inducing concentration was 50 µg/L, a concentration only 5 to 10 times higher than the highest environmental concentrations reported in the literature<sup>10,11</sup>. Since wild corals are exposed to solar filters for longer periods of time, it has been hypothesized that OC does impact corals in areas where it is continuously released. Other groups have also described the accumulation of UV filters in coral tissues<sup>8,12,13</sup>. These data further increase the interest of studying coral response to pollutants.

On July 2, 2018, and beginning January 1, 2021, Hawaii banned the sale or distribution of sunscreens containing oxybenzone or octinoxate in its territory<sup>14</sup>. Lately, Palau restricted the sale and use of reef-toxic sunscreens<sup>15</sup>. In that ruling, reef-toxic sunscreens were BP3, octinoxate and OC, the manufacturing, importation or sale of which will be prohibited in the Republic of Palau after January 1, 2020. In the current context, where national legislations are evolving to promote more sustainable tourism while little is known on the impact of UV filters on coral, it was key to evaluate more solar filters and to introduce a practical reliable tool to quantify coral responses to pollutants, while considering the public health importance of sunscreens.

In the current work, we studied the impact of 10 UV-filters on coral *Pocillopora damicornis* using untargeted metabolomic analysis in order to contribute to a better understanding of coral stress response to emerging pollutants.

## Results and discussion

---

### UV filters

The UV filters used in this study are listed in Table 1. All are approved in the European Union as cosmetic ingredients. Five of them are not approved by the FDA for human use but are often approved in other countries around the world, including those with significant coral reef areas such as France (4<sup>th</sup> most areas) and Australia (2<sup>nd</sup> most areas)<sup>16</sup>. Overall, the compound classes are somewhat diverse, with 5 classes for 10 solar filters.

**Table 1**

UV filters tested.

[Open in a separate window](#)<sup>a</sup> USA: United States of America, EU: European Union, Aus.: Australia. n.a.: not approved.

### Compared effect of OC and ES on coral metabolomes

In the current study, *P. damicornis* nubbins were exposed to ES for 7 days at concentrations of 5, 50, 300 and 1000 µg/L. As with OC previously, the extracts prepared from the coral nubbins exposed to ES were analyzed by UHPLC-ESI<sup>+</sup>-HRMS<sup>2</sup> and compared with control experiment<sup>7</sup>.

First, unlike what happened with OC, ES or ES-analogs do not seem to accumulate in the coral, although both compounds possess a 2-ethylhexyl side chain. Our hypothesis is that the ester group in OC is more stable than in ES. ES would then be degraded by carboxylesterase-mediated ester hydrolysis<sup>17</sup> or via the bacterial *ortho* degradation pathway<sup>18,19</sup>, while OC is degraded by hydroxylation of the 2-ethylhexyl chain and subsequent grafting of fatty acids. As a result, lipophilic OC analogs accumulate in coral tissues, which might lead to further accumulation by the trophic chain.

The metabolomic profiles were compared with those of control corals treated with DMSO only (0.25% v/v). Eighteen compounds are significantly upregulated at 1000 µg/L ES, and in some cases are also upregulated at lower ES concentrations (Table 2, Fig. 1).

**Table 2**

List of upregulated metabolites upon exposition to ES.

[Open in a separate window](#)

<sup>a</sup>Check marks indicate that the structure was confirmed by comparison with a commercial standard. For 14, see b.

<sup>b</sup>Structure confirmed by NMR.

<sup>c</sup>The molecular ion was not found, reported experimental *m/z* might correspond to a fragment.

[Open in a separate window](#)

### Figure 1

Identified upregulated metabolites and absolute integration values for biomarkers **1–18** ion peaks. The X-axis is in Log scale. For each ion, the leftmost point represents the minimal value, and the rightmost point the maximal one. The rectangular box represents the 25% quantile to 75% quantile ranges. The dark line shows the average of the distribution. Significance levels relative to DMSO were determined by an ANOVA followed by a Tukey HSD test. The differences were not significant unless otherwise stated. \*\*\* $p < 0.001$ , \*\* $p < 0.01$ , \* $p < 0.05$ .

Compounds **1–3** are the polyunsaturated fatty acids eicosapentaenoic, docosahexaenoic and arachidonic acid (AA, Fig. 1). The structures were determined based on the molecular formulas and examination of fragmentation spectra with MS-Finder. Identification was confirmed by comparison of retention times and MS/MS spectra with those of commercially available standards. These compounds were significantly upregulated at 1 mg/L ES and were not affected at lower concentrations (Fig. 1). Until recently,  $\omega$ 3 long-chain polyunsaturated fatty acids (PUFAs) would have been considered as Symbiodiniaceae<sup>20</sup> metabolites. Vertebrates lack the  $\omega$ x desaturases necessary for PUFA synthesis and it was largely accepted that all animals should lack it too. However, it is now well established that many marine invertebrates, including corals (*P. damicornis* among them), have acquired  $\omega$ x desaturases by horizontal gene transfer<sup>21,23</sup>.

In mammals,  $\omega$ 3 PUFAs, and in particular AA, that come from the diet are stored and are involved in the inflammatory cascade after cleavage from phosphatidylcholine by phospholipase A2 (PLA2) and transformation into several derived signaling molecules such as leukotrienes and prostaglandins. In corals, increased production of eicosanoids, linked to an increase in the expression of an allene oxide synthase-lipoxygenase (AOS-LOXa) was shown for the soft (octo)coral *Capnella imbricata* in response to mechanical injury and thermal stress<sup>22,24</sup>. In stony (hexa)corals, eicosanoids such as 8-hydroxyeicosatetraenoic acid (8-HETE), (S,5Z,11Z,14Z)-8-hydroxy-9-oxoicosa-5,11,14-trienoic acid and (5Z,12a,14Z)-9-oxo-prosta-5,10,14-trien-1-oic acid were also observed, both in extracts of whole coral tissue, and after incubation of <sup>14</sup>C-labeled AA with tissue homogenates of *Acropora millepora*, *A. cervicornis* and *Galaxea fascicularis*<sup>23</sup>. These results, combined with previous transcriptomic analysis showing upregulation of enzymes linked to eicosanoid production in corals undergoing black disease or thermal stress<sup>25,26</sup>, led to the hypothesis that the production of eicosanoids could also be associated with stress in stony corals<sup>23</sup>. Finally, experiments with host switching using the sea anemone *Exaiptasia pallida* also show evidences towards increases of eicoisanoids after colonization with a heterologous Symbiodiniaceae<sup>27</sup>.

Our *blastp* analysis of the *P. damicornis* genome identified several enzymes linked to the production of eicosanoids, including cytosolic and secreted PLA2, AOS-LOXs, 5-lipoxygenases and a leukotriene A4 hydrolase, confirming previous results in the literature (Supplementary Table S1)<sup>23,26</sup>. However, other than PUFAs, we could not detect any of the eicosanoids, leukotrienes or prostaglandins in *P. damicornis* extracts, nor could we identify a leukotriene receptor based on *blastp* searches using the mouse LTB4R and CYSLTR1 as queries. The closest seven-transmembrane G-protein coupled

receptors in *P. damicornis* were related to receptors in the alpha and beta groups of rhodopsin family (defined by Fredriksson *et al.*)<sup>28</sup> and not the gamma and delta groups as other known leukotriene receptors.

Altogether, these results suggest that  $\omega$ 3 PUFAs concentration increased likely in the context of a stress process triggered by ES. This effect was only noticeable at the highest exposition concentration, but the downstream signaling molecules or putative receptors were absent or not measurable in our study.

Compounds **4–7** have very similar MS/MS fragmentation patterns with common peaks at  $m/z$  60.0808 ( $[\text{Me}_3\text{NH}]^+$ ), 86.0964 ( $[\text{Me}_3\text{N}-\text{CH}=\text{CH}_2]^+$ ), 104.1070 ( $[\text{Me}_3\text{NCH}_2\text{CH}_2\text{OH}]^+$ ), 124.9998 ( $[\text{H}_2\text{O}_3\text{PO}-\text{CH}=\text{CH}_2]^+$ ), and 184.0733 ( $[\text{Me}_3\text{NCH}_2\text{CH}_2\text{OPO}_3\text{H}_2]^+$ ), showing evidence of the presence of a phosphocholine subunit (Supplementary Scheme S1). The molecular formula completed the structures as those of lysophosphatidylcholines (LPCs). In the collision-induced dissociation of sodiated **5** (Supplementary Fig. S14), the 5:1 peak intensity ratio of product ions at  $m/z$  104 and 147 indicated that **5** was an *sn*-1-LPC regioisomer<sup>29</sup>. The identification of compounds **5–7** was finally unambiguously established by comparing the retention times and MS/MS spectra with those of commercially available standards.

As for  $\omega$ 3 PUFAs, these compounds were significantly upregulated only at 1 mg/L ES (Fig. 1). LPCs are widespread in the animal kingdom<sup>30</sup>. In mammals, LPCs are proinflammatory lipids upregulated in an event of inflammation, inducing pro-inflammatory cytokine secretion and activating B lymphocytes<sup>31,33</sup>. LPCs stimulate time- and concentration-dependent release of arachidonic acid (compound **3**) in human coronary artery smooth muscle cells<sup>33</sup>. Interestingly, it has been proposed that the coral immune system is similar to that of higher organisms, including mammals<sup>34,37</sup>. In *Porites* sp., platelet-activating factor (PAF) concentration has been reported to increase during interactions with *Acropora cervicornis*<sup>30</sup> as has the expression of a gene coding for a putative LPC acetyltransferase, the protein responsible for converting LPC to PAF, in response to stress and inflammation in mammals<sup>38</sup>. PAF was not detected in our study, even though the genome of *P. damicornis* codes for an acyl transferase with high homology to the mammalian LPC acyltransferase, containing the motif HXXXXD responsible for acyltransferase activity, and a putative acyl-acceptor binding pocket domain (Supplementary Table S1). Remarkably, compound **7** is an isomer of PAF and could easily be mistaken for PAF. In our study, its structure was confirmed by comparison with standards of **7** and PAF (Supplementary Figs. S2 and S3). The fragmentation product at  $m/z$  104 from  $[\text{7} + \text{H}]^+$  further confirms the identification of **7** as the 1-*O*-octadecanoyl-*sn*-glycero-3-phosphocholine<sup>39,40</sup>. In addition, unlike what was reported for *Acropora digitifera*, we did not identify a gene coding PAF receptor based on *blastp* searches using the human PTAFR receptor as a query (Supplementary Table S1). The closest seven-transmembrane G-protein-coupled receptors in *P. damicornis* were related to cholecystokinin receptors in beta groups of the rhodopsin family (defined by Fredriksson *et al.*)<sup>28</sup> and not in the delta group as the PTAFR receptor. Finally, our results show that the expression of LPCs fluctuates widely between replicates (Fig. 1) and, therefore, cannot be considered as good stress indicators. The signal was weakly significant ( $p < 0.05$  for all 4 LPCs) at 1000  $\mu\text{g/L}$  ES and was not significant at lower concentrations.

Compounds **8–11** were identified as lysophosphatidylethanolamines (LPEs) based on molecular formulas, MS/MS fragmentation patterns, and structures proposed by CD for compounds **8–10**. Compounds **8** and **9** had very similar fragmentation patterns. For example, **8** is characterized by a series of products resulting from the successive loss of water ( $m/z$  464.3134), ethanolamine ( $m/z$

421.2731), and  $\text{HPO}_3$  ( $m/z$  341.3045, 100%) (Fig. 2, Supplementary Scheme S2). The ion at  $m/z$  310.3095 (330.2775 for **9**) corresponds to a product formed by transposition of the acyl unit to the amino group followed by  $\beta$ -elimination of the phosphate ester. This transposition only occurs for the *sn*-1-LPE regioisomers<sup>41</sup>. The structure of compound **9** was unambiguously confirmed by comparison with a commercial standard. The concentration of compounds **8** and **9** increased significantly at 300  $\mu\text{g/L}$  ES and above (Fig. 1). Compounds **10** and **11** are close analogs as demonstrated by their very similar  $\text{MS}^2$  fragmentation patterns, in which the migration of the enol ether chain on the amino group leads to the major fragmentation products (Fig. 3, Supplementary Scheme S3). The identification of compound **10** was confirmed by comparison with a commercially available standard. Compounds **10** and **11** were significantly upregulated at 1000  $\mu\text{g/L}$  ES.

[Figure 2](#)

Collision-induced MS/MS spectrum of the compound **9** pseudomolecular ion and identification of the key fragment ions.

[Open in a separate window](#)

[Figure 3](#)

Collision-induced MS/MS spectrum of the compound **11** pseudomolecular ion and identification of the key fragment ions.

[Open in a separate window](#)

It has been well established that LPEs and LPCs are produced by hydrolysis of phosphatidylethanolamines and phosphatidylcholines, releasing arachidonic acid or other fatty acids linked to the *sn*-2 position. This reaction is usually mediated by a phospholipase A2. An increased phospholipase A2 activity in coral exposed to ES would account for the observed concomitant increase of  $\omega$ 3 PUFAs (**1–3**), LPCs (**4–7**) and LPEs (**8–11**). As discussed above *P. damicornis* genome mining revealed that the genome of this species codes for a number of secretory (sPLA2) and cytosolic PLA2 (cPLA2) presumably involved in this mechanism. Similar to in mammals<sup>42,43</sup>, sPLA2 upregulation in coral is visibly associated with the activity of the innate immune system and/or a stress response<sup>26,38</sup>. Increases in PLA2 expression and arachidonic acid was also shown after host switching with a heterologous Symbiodiniaceae with sea anemone *Exaiptasia pallida* even though that study did not see differences in LPEs and LPCs<sup>27</sup>. Overall, the metabolomic response of coral after exposition to ES resembles the signature of a stress/inflammatory process triggered by ES.



To the exception of compound **14**, compounds **12–17** (Fig. [1](#)) were detected with somewhat small response peaks, and it was not always possible to obtain MS/MS spectra. Compounds **12–17** seemed related based on their molecular formulas and on their ionization and fragmentation patterns. Interestingly, the differential analysis showed that all these compounds were significantly upregulated when the coral was exposed to ES at concentrations ranging from 50 to 1000  $\mu\text{g/L}$ . It turned out that the concentration of **14** also increased upon exposition to OC<sup>[7](#)</sup>, and at this point, it was clearly necessary to determine unambiguously the structure of compound **14**. Extensive fractionation allowed for the isolation of **14** in its pure form, which was ultimately identified by NMR as the known steroid (3 $\beta$ ,5 $\alpha$ ,8 $\alpha$ )-5, 8-epidioxy-ergosta-6,24(28)-dien-3-ol. Compound **14** along with many epidioxy sterol analogs have been described essentially in marine invertebrates, including several cnidarians<sup>[44](#), [47](#)</sup>. The role and fate of this compound in invertebrates remains an unresolved question. However, steroids are present in the whole animal kingdom. They regulate life cycles, mating, and development. In Cnidarians, bioregulatory pathways and hormonal-like signaling remain largely uncharacterized<sup>[48](#), [50](#)</sup>. Nonetheless, a family of nuclear receptors has been found to bind the ancient hormone paraestrol A<sup>[50](#), [51](#)</sup>. According to Khalturin *et al.*, Cnidarian steroids can be transported in the digestive tract and through the mesoglea, and may be involved in intercellular communication. Here, compound **14** concentration increased in coral exposed to pollutants, and these pollutants eventually triggered a stress response witnessed by the increased production of specific lipids. We hypothesize that the increased concentration of this class of steroids – and in particular the major compound **14** – is a signal triggering a coral inflammatory-like response. Owing to the very small standard deviation within replicates (Fig. [2](#)), **14** could be considered as a good marker of stressed corals. In our experiments, the concentration of **14** significantly increased with both ES and OC at 50  $\mu\text{g/L}$ , indicating that both solar filters had a negative impact on coral. However, ES triggered a stress/inflammatory response while OC also specifically altered mitochondrial function<sup>[7](#)</sup>.

Last, it should be mentioned that the relative concentration of five metabolites decreased when the coral was exposed to ES at 1 mg/L (Supplementary Figs. [S1](#), [S51](#)–[S61](#)). These metabolites have been identified as four monogalactosyl diacylglycerols (MGDGs **19–22**) and one cerebroside (**23**). In MS<sup>2</sup>, MGDG fragmentation pattern shows the length and number of unsaturation of each acyl chain. The relative position of the acyl chains can be assigned based on the relative peak intensities of the sodium adduct fragmentation products. The peak intensity of the product ion resulting from the loss of the *sn*-1 fatty acid is always higher than the one resulting from the loss of the *sn*-2 fatty acid<sup>[52](#)</sup>. Although cerebroside is widely distributed in the eukaryotes, galactolipids including MGDGs are the main components of plant chloroplast membrane lipids<sup>[53](#), [54](#)</sup>. Decreased MGDGs concentration might point towards an effect of the UV filter on the coral symbiont. It is possible that the coral had begun to bleach although bleaching was not visible to the naked eye. However, specific toxicity mechanism unbalancing Symbiodiniaceae metabolism or any process disrupting algal symbiont metabolite translocation cannot be ruled out.

### Effect of BEMT, BM, BP3, DBT, DHHB, ET, HS, and MBBT

The effect of 8 other solar filters was examined based on the comparison of global metabolomic profiles between exposed and unexposed coral, but it was also examined in light of the putative increased concentration of compound **14** in exposed corals. In general, the first step consisted of exposing coral at 1000  $\mu\text{g/L}$  of each solar filter and testing lower concentrations when an effect was

detected. BP3 was tested at 2000  $\mu\text{g/L}$  as well because very high environmental concentrations of this compound have been occasionally detected<sup>3</sup>. The relative variations in compound **14** concentration are reported in Fig. 4.

**Figure 4**

Relative integration values for compound **14** ion peak in exposed coral compared to control animals. The vertical dashed line illustrates the 1:1 ratio. The rectangular box represents the min to max ranges. The dark line shows the average of the distribution. Significance levels relative to DMSO were determined by an ANOVA followed by a Tukey HSD test. The differences were not significant unless otherwise stated. \*\*\* $p < 0.001$ , \*\* $p < 0.01$ , \* $p < 0.05$ . The multiple data points for same concentrations are for repeat experiments.

[Open in a separate window](#)

We observed that BEMT, DBT, DHHB, ET and MBBT do not seem to affect the overall coral metabolome at the highest concentration tested. Specific measurement of the concentration of compound **14** in treated versus untreated coral confirmed the apparent innocuousness of these five molecules, as the concentration of **14** remained stable. It was found that the concentration of **14** increased at 2 mg/L BP3, indicating that BP3 most certainly affects wild coral at the highest published environmental concentration<sup>3</sup>. Coral exposure to BM does not induce an increase in the concentration of compound **14**. Nevertheless, the presence of undetermined ions in the global coral metabolome will require further investigation. Last, HS does not alter either the concentration of compound **14** or the overall metabolome of *P. damicornis*. However, polyps of coral exposed to HS at 1 mg/L were closed at the end of the assay, while those of control corals were not, as if the coral reacted although its metabolome was not significantly altered (Supplementary Fig. [S61](#)).

## Conclusion

This work establishes a metabolomic signature of stressed *P. damicornis*. In this coral, the known steroid (3 $\beta$ , 5 $\alpha$ , 8 $\alpha$ )-5,8-epidioxy-ergosta-6,24(28)-dien-3-ol (**14**) is viewed as a steroid hormone that could trigger coral response to pollutants. OC was the most toxic of the tested UV filters. It induced coral stress response, while triggering mitochondrial dysfunction at 50  $\mu\text{g/L}$ . Of concern was also the previously reported accumulation potential of possibly toxic coral-modified OC derivatives. ES comes second in terms of toxicity. ES triggered coral stress response at 50  $\mu\text{g/L}$ , inducing a significant increase in the concentration of compound **14**. At 300  $\mu\text{g/L}$  ES and above, the relative concentration of several PUFAs, LPCs and LPAs also increased. ES may also have induced partial coral bleaching at 1 mg/L although this remains to be firmly established. BP3 was also toxic at 2 mg/L in our assay. BEMT, BM, DBT, DHHB, ET, HS and MBBT did not affect coral metabolism at any of the concentrations tested, although in the case of HS and BM, further investigations are needed to evaluate their potential effects. More investigations are also needed to clarify the role of compound **14** in coral hormonal response to pollutants.

## Methods



## General experimental procedures

Nuclear Magnetic Resonance (NMR) spectra were recorded on a JEOL ECZ500R spectrometer equipped with a 5-mm inverse detection FG/RO Digital Autotune Probe. Chemical shifts ( $\delta$ ) are reported as ppm downfield from tetramethylsilane, and the coupling constants ( $J$ ) are reported in Hertz. High-resolution MS/MS analyses were conducted with a Thermo UHPLC-HRMS system<sup>7</sup>. Analyses were performed in the electrospray positive ionization mode in the range of 133.4–2000 Da in the centroid mode. The mass detector was an Orbitrap MS/MS FT Q-Exactive focus mass spectrometer. The analyses were conducted in FullMS-data dependent MS<sup>2</sup> mode. In FullMS, the resolution was set to 70,000, and the AGC target was  $3.10^6$ . In MS<sup>2</sup>, the resolution was 17,500, AGC target  $10^5$ , isolation window 0.4 Da, and stepped normalized collision energy 15/30/45 was used, with 15 s dynamic exclusion. The lock mass option was set for an ion at  $m/z$  144.98215, corresponding to  $\text{Cu}(\text{CH}_3\text{CN})_2^+$ . For coral profiling and comparison of coral profiles with standards, the UHPLC column was a Phenomenex Luna Omega polar C-18  $150 \times 2.1$  mm,  $1.6 \mu\text{m}$ . The column temperature was set to  $42^\circ\text{C}$ , and the flow rate was  $0.5 \text{ mL}\cdot\text{min}^{-1}$ . The solvent system was a mixture of water (solution A) with increasing proportions of acetonitrile (solution B), and both solvents were modified with 0.1% formic acid. The gradient was as follows: 2% B 3 min before injection; then from 1 to 13 min, there was a shark fin gradient increase of B up to 100% (curve 2), followed by 100% B for 5 min. The flow was diverted (not injected into the mass spectrometer) before injection, up to 1 min after injection. For fast analysis of the fractions of coral extract, the UHPLC column was a Thermo Scientific Accucore Vanquish C18 + 50  $\times 2.1$  mm,  $1.5 \mu\text{m}$ . The column temperature was set to  $42^\circ\text{C}$ , and the flow rate was  $0.5 \text{ mL}\cdot\text{min}^{-1}$ . The gradient was as follows: 2% B 1 min before injection; then from 0 to 4 min, there was a shark fin gradient increase of B up to 100% (curve 2), followed by 100% B for 1 min. The flash chromatography was performed with a Teledyne ISCO CombiFlash Companion equipped with a Büchi FlashPure Ecoflex C18  $50 \mu\text{m}$  40 g column. The column was equilibrated with water: $\text{CH}_3\text{CN}$  4:6. The flow rate was 40 mL/min. The injection was performed in the solid phase, with fraction F3 impregnated on C18 silica (1 mL). The gradient was 60% acetonitrile until 1 min after injection; then, from 1 to 20 min, there was a linear gradient increase of acetonitrile up to 100%, followed by 100% acetonitrile for 10 min. Effluents were collected in 30 s fractions. The preparative HPLC was conducted with a hybrid system mounted with a Reodyne manual injector, 2 Varian PrepStar 218 HPLC pumps, a Dionex Ultimate 3000 variable wavelength detector, and a Dionex Ultimate 3000 fraction collector. The column was a Phenomenex Luna C18  $250 \times 21.20$  mm,  $5 \mu\text{m}$ . The gradient was as follows: 90% acetonitrile from 0 to 8 min, 91% from 8 to 16 min, 92% from 16 to 32 min, and 100% for 13 min. The flow rate was 20 mL/min, and fractions were collected every 30 s. The second preparative HPLC was performed on small scale with a Dionex ultimate 3000 system equipped with a deaerator, an HPG-3200SD pumping device, an autosampler, a column oven, a diode array detector and a fraction collector. The column was a Phenomenex Luna C18  $150 \times 4.60$  mm,  $5 \mu\text{m}$ . The solvent was an isocratic mixture of water: $\text{CH}_3\text{CN}$  15:85 modified with 0.1% formic acid. The flow rate was 1 mL/min, and fractions were collected every 30 s.

## Chemicals

The solar filters used in this study are listed in Table 1. BEMT, BM, BP3, and MBBT were purchased from Sigma-Aldrich, Saint-Quentin Fallavier, France. DBT, DHHB, ES, ET, HS, and OC were provided by Pierre Fabre Laboratories. Standards of platelet-activating factor (PAF) and compounds 1–3, 5–7, 9, and 11 were purchased from AnalyticLab, Montpellier, France.

Fragments of the coral *P. damicornis* were collected in Oman in 2014 (CITES permit 37/2014). This procedure had no impact on the wild population as 1–5% of few coral colonies were collected. The coral was acclimated in tanks at the Banyuls Oceanological Observatory. New colonies were obtained in the laboratory from the fragments and used for our experiments. The corals were maintained in artificial sea water (ASW) prepared with reverse osmosis purified water and Reef Salt SeaChem salts. Salinity was adjusted to 36 g/L, pH = 8, and the temperature was set at 24 °C. All experiments were conducted with the same ASW.

### Exposition of coral to solar filters, extraction and metabolomic analyses

The coral exposition protocol, the extraction, the metabolomic profiling and the statistical analyses were conducted as described before for OC<sup>7</sup>. They are also reported in Supplementary Information. Five replicates were used for each condition, and in some cases, the conditions were repeated. The standard compounds were diluted in MeOH ( $\approx 10 \mu\text{g/mL}$  each,  $1 \mu\text{L}$  injected) and were analyzed in the same conditions as the coral extracts for comparison of retention times, MS and MS/MS spectra. All standards were identical to the coral metabolites in retention times and MS/MS spectra (see supplementary information). Interpretations of the metabolomic data and MS/MS spectra were conducted with the help of Compound Discoverer 2.1 and FreeStyle 1.3 (Thermo Fisher Scientific, Villebon, France), and MS-Finder 3.04<sup>55,56</sup>. The same procedure as in Stien *et al.* (2019) was used for Compound Discover. Extracted ion chromatograms for compounds **1–18** along with ESI<sup>+</sup>-HRMS spectra, collision-induced dissociation spectra and comparison with commercial standards are provided in Supporting Information (Supplementary Figs. [S4–S50](#)).

### Isolation and characterization of compound 14

Approximately 200 2–5 cm-long coral nubbins were cut from the branch tips of mother colonies. The nubbins were placed in a large Erlenmeyer flask and covered with MeOH:CH<sub>3</sub>CN 1:1. After 24 h at room temperature, the flask was sonicated for 20 min, the coral pieces were removed by filtration, and the solvent was evaporated to give the crude coral extract (2.5 g). The crude extract was dissolved in the smallest amount DMSO possible and was purified by SPE with a phenomenex Strata C-18 150 mL column. The column was equilibrated successively with CH<sub>3</sub>CN and water. Elution was performed with water (300 mL, F1), with water:CH<sub>3</sub>CN 1:1 (300 mL, F2) and finally with MeOH:CH<sub>2</sub>Cl<sub>2</sub> 8:2 (300 mL, F3). Fractions were evaporated and diluted in MeOH at 1 mg/mL for LC/MS analyses ( $1 \mu\text{L}$  injected). The target compound at  $t_R \approx 11.02$  min and  $m/z$  395.3308 was detected in fraction F3 (0.29 g). Fraction F3 was purified by flash chromatography, providing 80 fractions. The analysis of the fractions demonstrated that the target compound was detected in fractions 45 to 63. These fractions were gathered and evaporated. For injection, fraction F3.45–63 (49.95 mg) was diluted in water:CH<sub>3</sub>CN 1:9 (2 mL). Preparative HPLC was performed twice with 1 mL injected. The targeted compound was concentrated in fractions 40 to 45, which were gathered and evaporated. The resulting fraction F3.45-63.40-45 (5.91 mg) was diluted in water:CH<sub>3</sub>CN 15:85 (1.5 mL) and was purified by small-scale preparative HPLC by portions of 250  $\mu\text{L}$  (6 injections). The desired compound **14** was isolated in pure form from fractions 27–29 (0.9 mg).

### Analytical data for compound 14

5 $\alpha$ ,8 $\alpha$ -Epidioxysterosta-6,24(28)-dien-3 $\beta$ -ol (**14**).  $^1\text{H}$  NMR (500 MHz,  $\text{CDCl}_3$ ):  $\delta$  0.81 (s, 3 H, H-18), 0.88 (s, 3 H, H-19), 0.94 (d, 3 H,  $J$  = 6.5 Hz, H-21), 1.02 (d, 3 H,  $J$  = 6.8 Hz, H-26), 1.03 (d, 3 H,  $J$  = 6.8 Hz, H-27), 1.21 (m, 1 H, H-17), 1.16 (m, 1 H, H-22a), 1.22 (m, 1 H, H-11a), 1.23 (m, 1 H, H-12a), 1.39 (m, 1 H, H-16a), 1.408 (m, 1 H, H-15a), 1.411 (m, 1 H, H-20), 1.22 (m, 1 H, H-11a), 1.496 (m, 1 H, H-9), 1.497 (m, 1 H, H-11b), 1.53 (m, 1 H, H-2a), 1.54 (m, 1 H, H-22b), 1.55 (m, 1 H, H-14), 1.63 (m, 1 H, H-15b), 1.69 (dt, 1 H,  $J$  = 13.5, 3.4 Hz, H-1a), 1.85 (m, 1 H, H-2b), 1.89 (m, 1 H, H-23a), 1.94 (m, 1 H, H-16b), 1.95 (m, 1 H, H-1b), 1.98 (m, 1 H, H-12b), 1.91 (dd, 1 H,  $J$  = 13.9, 11.7 Hz, H-4a), 2.09 (brdd, 1 H,  $J$  = 10.9, 4.7 Hz, H-23b), 2.11 (ddd, 1 H,  $J$  = 13.9, 4.9, 1.9 Hz, H-4b), 2.22 (heptd, 1 H,  $J$  = 6.8, 1.0 Hz, H-25), 3.97 (m, 1 H, H-3), 4.65 (brq, 1 H,  $J$  = 1.4 Hz, H-28a), 4.72 (brs, 1 H, H-28b), 6.24 (d, 1 H,  $J$  = 8.5 Hz, H-6), 6.51 (d, 1 H,  $J$  = 8.5 Hz, H-7);  $^{13}\text{C}$  NMR (125 MHz,  $\text{CDCl}_3$ ):  $\delta$  12.6 (C-18), 18.2 (C-19), 18.6 (C-21), 20.6 (C-15), 21.8 (C-27), 22.0 (C-26), 23.4 (C-11), 28.2 (C-16), 30.1 (C-2), 30.9 (C-23), 33.8 (C-25), 34.4 (C-22), 34.7 (C-1), 35.2 (C-20), 36.9 (C10), 37.0 (C-4), 39.4 (C-12), 44.7 (C-13), 51.1 (C-6), 51.6 (C-14), 56.3 (C-17), 66.5 (C-3), 106.1 (C-28), 130.7 (C-7), 135.4 (C-6), 156.6 (C-24); HR-ESI $^+$ -MS  $m/z$  found 429.3362  $[\text{M} + \text{H}]^+$ ; calcd. for  $[\text{C}_{28}\text{H}_{45}\text{O}_3]^+$ : 429.3363; HR-ESI $^+$ -MS  $m/z$  395.3307 (100,  $[\text{M} + \text{H} - \text{H}_2\text{O}_2]^+$ ), 429.3361 (41,  $[\text{M} + \text{H}]^+$ ), 377.3202 (41,  $[\text{M} + \text{H} - \text{H}_2\text{O}_2 - \text{H}_2\text{O}]^+$ ), 411.3255 (24,  $[\text{M} + \text{H} - \text{H}_2\text{O}]^+$ ), 451.3180 (8,  $[\text{M} + \text{Na}]^+$ ); HR-ESI $^+$ -MS $^2$  for  $[\text{M} + \text{H}]^+$  ion  $m/z$  429.3357 (100), 81.0698 (45), 411.3251 (43), 95.0854 (33), 107.0853 (22), 69.0698 (21), 109.1011 (20).

### *P. damicornis* genome mining

To interpret the possible roles of the identified stress biomarkers, we queried a number of possible putative enzymes and receptors leading to the synthesis, modification and binding of different phospholipids, polyunsaturated fatty acids and oxylipins against proteins coded by the *P. damicornis* genome [NCBI genome 22550, ASM380409v1 reference annotation release 100/annotated proteins<sup>36</sup>] using the web-based *blastp* program of the NCBI and default parameters. Reciprocal *blastp* searches were also conducted using the web-based tool against the *UniProt/Swiss-Prot*, and *model organism (landmark)* databases, and in some specific cases, the conserved domains (CDD) search. Query sequences for putative enzymes were retrieved by text searches in the MetaCyc, Brenda and KEGG databases, and whenever possible, the closest (based on phylogenetic proximity) experimentally validated sequences were used. Receptor sequences for queries were identified by text searches in the GLASS-GPCR (<https://zhanglab.ccmb.med.umich.edu/GLASS/index.html>) database using the same selection criterion as for the enzymes.

### Supplementary information

[Supplementary information](#). (2.7M, pdf)

### Acknowledgements

We thank the BIO2MAR platform (<http://bio2mar.obs-banyuls.fr>) for providing technical support and access to instrumentation. We thank the Pierre Fabre Laboratories for financial sponsorship to the laboratory, and the European Marine Biological Resource Center (EMBRC) at the Observatoire Océanologique de Banyuls, France, for providing access to the Banyuls aquarium facilities. Finally, the authors would like to thank Rémi Pillot and Pascal Romans (Sorbonne Université) for their help in developing the coral assay.

## Author contributions

D.S. and P.L. conceived the work. A.M.S.R. and M.Y. isolated compound **14**. F.C. and E.T. performed coral exposition to UV filters. D.S. conducted metabolomic profiling, analyzed LC-MS and NMR data, and prepared the manuscript including figures and tables. M.S. performed *P. damicornis* genome mining and amended the manuscript accordingly. All authors corrected the manuscript and have given approval to the final version.

## Competing interests

The work reported in this article was financed in the context of the Pierre Fabre Skin Protect Ocean Respect action. It was neither supervised nor audited by Pierre Fabre Laboratories. The interpretation and views expressed in this manuscript are not those of the company.

## Footnotes

**Publisher's note** Springer Nature remains neutral with regard to jurisdictional claims in published maps and institutional affiliations.

## Supplementary information

is available for this paper at 10.1038/s41598-020-66117-3.

## References

1. Pandolfi JM, et al. Global trajectories of the long-term decline of coral reef ecosystems. *Science* (80-.). 2003;301:955–958. [[PubMed](#)] [[Google Scholar](#)]
2. Danovaro R, et al. Sunscreens cause coral bleaching by promoting viral infections. *Environ. Health Perspect.* 2008;116:441–447. [[PMC free article](#)] [[PubMed](#)] [[Google Scholar](#)]
3. Downs CA, et al. Toxicopathological effects of the sunscreen UV filter, oxybenzone (benzophenone-3), on coral planulae and cultured primary cells and its environmental contamination in Hawaii and the U.S. Virgin Islands. *Arch. Environ. Contam. Toxicol.* 2016;70:265–288. [[PubMed](#)] [[Google Scholar](#)]
4. DiNardo JC, Downs CA. Dermatological and environmental toxicological impact of the sunscreen ingredient oxybenzone/benzophenone-3. *J. Cosmet. Dermatol.* 2018;17:15–19. [[PubMed](#)] [[Google Scholar](#)]
5. Downs CA, et al. Toxicological effects of the sunscreen UV filter, benzophenone-2, on planulae and *in vitro* cells of the coral, *Stylophora pistillata*. *Ecotoxicology.* 2014;23:175–191. [[PubMed](#)] [[Google Scholar](#)]
6. He T, et al. Comparative toxicities of four benzophenone ultraviolet filters to two life stages of two coral species. *Sci. Total Environ.* 2019;651:2391–2399. [[PubMed](#)] [[Google Scholar](#)]
7. Stien D, et al. Metabolomics reveal that octocrylene accumulates in *Pocillopora damicornis* tissues as fatty acid conjugates and triggers coral cell mitochondrial dysfunction. *Anal. Chem.* 2019;91:990–995. [[PubMed](#)] [[Google Scholar](#)]
8. He T, et al. Toxicological effects of two organic ultraviolet filters and a related commercial sunscreen product in adult corals. *Environ. Pollut.* 2019;245:462–471. [[PubMed](#)] [[Google Scholar](#)]

9. Fel J-P, et al. Photochemical response of the scleractinian coral *Stylophora pistillata* to some sunscreen ingredients. *Coral Reefs*. 2019;38:109–122. [[Google Scholar](#)]
10. Tsui MMP, et al. Occurrence, distribution and ecological risk assessment of multiple classes of UV filters in surface waters from different countries. *Water Res*. 2014;67:55–65. [[PubMed](#)] [[Google Scholar](#)]
11. Langford KH, Reid MJ, Fjeld E, Øxnevad S, Thomas KV. Environmental occurrence and risk of organic UV filters and stabilizers in multiple matrices in Norway. *Environ. Int*. 2015;80:1–7. [[PubMed](#)] [[Google Scholar](#)]
12. Mitchelmore CL, et al. Occurrence and distribution of UV-filters and other anthropogenic contaminants in coastal surface water, sediment, and coral tissue from Hawaii. *Sci. Total Environ*. 2019;670:398–410. [[PubMed](#)] [[Google Scholar](#)]
13. Tsui MMP, et al. Occurrence, distribution, and fate of organic UV filters in coral communities. *Environ. Sci. Technol*. 2017;51:4182–4190. [[PubMed](#)] [[Google Scholar](#)]
14. State of Hawaii. Senate Bill No. 2571, S.D. 2, H.D. 2, C.D. 1. (2018). Available at, [https://www.capitol.hawaii.gov/session2018/bills/SB2571\\_CD1\\_.HTM](https://www.capitol.hawaii.gov/session2018/bills/SB2571_CD1_.HTM). (Accessed: 27th June 2019).
15. Republic of Palau. Senate Bill No. 10-135, SD1, HD1 (The Responsible Tourism Education Act of 2018). (2018). Available at, <http://www.palau.gov.pw/wp-content/uploads/2018/10/RPPL-No.-10-30-re.-The-Responsible-Tourism-Education-Act-of-2018.pdf>. (Accessed: 27th June 2019).
16. Spalding, M. D., Ravilious, C. & Green, E. P. World atlas of coral reefs. (University of California Press, 2001), doi 10.1016/S0025-326×(01)00310-1
17. Belsito D, et al. A toxicologic and dermatologic assessment of salicylates when used as fragrance ingredients. *Food Chem. Toxicol*. 2007;45:S318–S361. [[PubMed](#)] [[Google Scholar](#)]
18. Oie CSI, Albaugh CE, Peyton BM. Benzoate and salicylate degradation by *Halomonas campisalis*, an alkaliphilic and moderately halophilic microorganism. *Water Res*. 2007;41:1235–1242. [[PubMed](#)] [[Google Scholar](#)]
19. Sazonova OI, Izmalkova TY, Kosheleva IA, Boronin AM. Salicylate degradation by *Pseudomonas putida* strains not involving the “Classical” *nah2* operon. *Microbiology*. 2008;77:710–716. [[PubMed](#)] [[Google Scholar](#)]
20. LaJeunesse TC, et al. Systematic revision of Symbiodiniaceae highlights the antiquity and diversity of coral endosymbionts. *Curr. Biol*. 2018;28:2570–2580. [[PubMed](#)] [[Google Scholar](#)]
21. Kabeya N, et al. Genes for de novo biosynthesis of omega-3 polyunsaturated fatty acids are widespread in animals. *Sci. Adv*. 2018;4:eaar6849. [[PMC free article](#)] [[PubMed](#)] [[Google Scholar](#)]
22. Löhelaïd H, Teder T, Töldsepp K, Ekins M, Samel N. Up-regulated expression of AOS-LOXa and increased eicosanoid synthesis in response to coral wounding. *PLoS One*. 2014;9:e89215. [[PMC free article](#)] [[PubMed](#)] [[Google Scholar](#)]
23. Löhelaïd H, Samel N, Löhelaïd H, Samel N. Eicosanoid diversity of stony corals. *Mar. Drugs*. 2018;16:10. [[PMC free article](#)] [[PubMed](#)] [[Google Scholar](#)]



24. Löhela H, Teder T, Samel N. Lipoxigenase-allene oxide synthase pathway in octocoral thermal stress response. *Coral Reefs*. 2015;34:143–154. [[Google Scholar](#)]
25. Libro S, Kaluziak ST, Vollmer SV. RNA-seq profiles of immune related genes in the staghorn coral *Acropora cervicornis* infected with white band disease. *PLoS One*. 2013;8:e81821. [[PMC free article](#)] [[PubMed](#)] [[Google Scholar](#)]
26. Vidal-Dupiol J, et al. Thermal stress triggers broad *Pocillopora damicornis* transcriptomic remodeling, while *Vibrio coralliilyticus* infection induces a more targeted immuno-suppression response. *PLoS One*. 2014;9:e107672. [[PMC free article](#)] [[PubMed](#)] [[Google Scholar](#)]
27. Matthews JL, et al. Optimal nutrient exchange and immune responses operate in partner specificity in the cnidarian-dinoflagellate symbiosis. *Proc. Natl. Acad. Sci.* 2017;114:13194–13199. [[PMC free article](#)] [[PubMed](#)] [[Google Scholar](#)]
28. Fredriksson R, Lagerström MC, Lundin L-G, Schiöth HB. The G-protein-coupled receptors in the human genome form five main families. Phylogenetic analysis, paralogon groups, and fingerprints. *Mol. Pharmacol.* 2003;63:1256–1272. [[PubMed](#)] [[Google Scholar](#)]
29. Han X, Gross RW. Structural determination of lysophospholipid regioisomers by electrospray ionization tandem mass spectrometry. *J. Am. Chem. Soc.* 1996;118:451–457. [[Google Scholar](#)]
30. Galtier d'Auriac I, et al. Before platelets: the production of platelet-activating factor during growth and stress in a basal marine organism. *Proc. R. Soc. B Biol. Sci.* 2018;285:20181307. [[PMC free article](#)] [[PubMed](#)] [[Google Scholar](#)]
31. Bansal P, Gaur SN, Arora N. Lysophosphatidylcholine plays critical role in allergic airway disease manifestation. *Sci. Rep.* 2016;6:27430. [[PMC free article](#)] [[PubMed](#)] [[Google Scholar](#)]
32. Huang YH, Schäfer-Elinder L, Wu R, Claesson HE, Frostegård J. Lysophosphatidylcholine (LPC) induces proinflammatory cytokines by a platelet-activating factor (PAF) receptor-dependent mechanism. *Clin. Exp. Immunol.* 1999;116:326–331. [[PMC free article](#)] [[PubMed](#)] [[Google Scholar](#)]
33. Aiyar N, et al. Lysophosphatidylcholine induces inflammatory activation of human coronary artery smooth muscle cells. *Mol. Cell. Biochem.* 2007;295:113–120. [[PubMed](#)] [[Google Scholar](#)]
34. Palmer CV, Traylor-Knowles NG, Willis BL, Bythell JC. Corals use similar immune cells and wound-healing processes as those of higher organisms. *PLoS One*. 2011;6:e23992. [[PMC free article](#)] [[PubMed](#)] [[Google Scholar](#)]
35. Palmer CV, Traylor-Knowles N. Towards an integrated network of coral immune mechanisms. *Proc. R. Soc. B Biol. Sci.* 2012;279:4106–4114. [[PMC free article](#)] [[PubMed](#)] [[Google Scholar](#)]
36. Cuning R, Bay RA, Gillette P, Baker AC, Traylor-Knowles N. Comparative analysis of the *Pocillopora damicornis* genome highlights role of immune system in coral evolution. *Sci. Rep.* 2018;8:16134. [[PMC free article](#)] [[PubMed](#)] [[Google Scholar](#)]
37. van de Water JAJM, et al. The coral immune response facilitates protection against microbes during tissue regeneration. *Mol. Ecol.* 2015;24:3390–3404. [[PubMed](#)] [[Google Scholar](#)]
38. Quinn RA, et al. Metabolomics of reef benthic interactions reveals a bioactive lipid involved in coral defence. *Proc. R. Soc. B Biol. Sci.* 2016;283:20160469. [[PMC free article](#)] [[PubMed](#)] [[Google Scholar](#)]



39. Rizea Savu S, et al. Determination of 1-*O*-acyl-2-acetyl-*sn*-glyceryl-3-phosphorylcholine, platelet-activating factor and related phospholipids in biological samples by high-performance liquid chromatography-tandem mass spectrometry. *J. Chromatogr. B Biomed. Sci. Appl.* 1996;682:35–45. [[PubMed](#)] [[Google Scholar](#)]
40. Kim SJ, Back SH, Koh JM, Yoo HJ. Quantitative determination of major platelet activating factors from human plasma. *Anal. Bioanal. Chem.* 2014;406:3111–3118. [[PubMed](#)] [[Google Scholar](#)]
41. Lau S, et al. Metabolomic profiling of plasma from melioidosis patients using UHPLC-QTOF MS reveals novel biomarkers for diagnosis. *Int. J. Mol. Sci.* 2016;17:307. [[PMC free article](#)] [[PubMed](#)] [[Google Scholar](#)]
42. Masuda S, et al. Various secretory phospholipase A2 enzymes are expressed in rheumatoid arthritis and augment prostaglandin production in cultured synovial cells. *FEBS J.* 2005;272:655–672. [[PubMed](#)] [[Google Scholar](#)]
43. Triggiani M, Granata F, Giannattasio G, Marone G. Secretory phospholipases A2 in inflammatory and allergic diseases: Not just enzymes. *J. Allergy Clin. Immunol.* 2005;116:1000–1006. [[PubMed](#)] [[Google Scholar](#)]
44. Gunatilaka AAL, Gopichand Y, Schmitz FJ, Djerassi C. Minor and trace sterols in marine invertebrates. 26. Isolation and structure elucidation of nine new 5 $\alpha$ ,8 $\alpha$ -epidoxysterols from four marine organisms. *J. Org. Chem.* 1981;46:3860–3866. [[Google Scholar](#)]
45. Stonard RJ, Petrovich JC, Andersen RJ. A new C26 sterol peroxide from the opisthobranch mollusk *Adalaria* sp. and the sea pen *Virgularia* sp. *Steroids.* 1980;36:81–86. [[PubMed](#)] [[Google Scholar](#)]
46. Findlay JA, Patil AD. A novel sterol peroxide from the sea anenome *Metridium senile*. *Steroids.* 1984;44:261–265. [[PubMed](#)] [[Google Scholar](#)]
47. Ioannou E, et al. 5 $\alpha$ ,8 $\alpha$ -Epidioxysterols from the gorgonian *Eunicella cavolini* and the ascidian *Trididemnum inarmatum*: Isolation and evaluation of their antiproliferative activity. *Steroids.* 2009;74:73–80. [[PubMed](#)] [[Google Scholar](#)]
48. Tarrant AM. Hormonal signaling in cnidarians: Do we understand the pathways well enough to know whether they are being disrupted? *Ecotoxicology.* 2007;16:5–13. [[PubMed](#)] [[Google Scholar](#)]
49. Tarrant AM. Endocrine-like signaling in cnidarians: Current understanding and implications for ecophysiology. *Integr. Comp. Biol.* 2005;45:201–2014. [[PubMed](#)] [[Google Scholar](#)]
50. Khalturin K, et al. NR3E receptors in cnidarians: A new family of steroid receptor relatives extends the possible mechanisms for ligand binding. *J. Steroid Biochem. Mol. Biol.* 2018;184:11–19. [[PMC free article](#)] [[PubMed](#)] [[Google Scholar](#)]
51. Markov GV, et al. Origin of an ancient hormone/receptor couple revealed by resurrection of an ancestral estrogen. *Sci. Adv.* 2017;3:e1601778. [[PMC free article](#)] [[PubMed](#)] [[Google Scholar](#)]
52. Guella G, Frassanito R, Mancini I. A new solution for an old problem: The regiochemical distribution of the acyl chains in galactolipids can be established by electrospray ionization tandem mass spectrometry. *Rapid Commun. Mass Spectrom.* 2003;17:1982–1994. [[PubMed](#)] [[Google Scholar](#)]
53. Joyard J, et al. The biochemical machinery of plastid envelope membranes. *Plant Physiol.* 1998;118:715–723. [[PMC free article](#)] [[PubMed](#)] [[Google Scholar](#)]

54. Marcellin-Gros R, Piganeau G, Stien D. Metabolomic insights into marine phytoplankton diversity. *Mar. Drugs*. 2020;18:78. [[PMC free article](#)] [[PubMed](#)] [[Google Scholar](#)]
55. Tsugawa H, et al. Hydrogen rearrangement rules: Computational MS/MS fragmentation and structure elucidation using MS-FINDER software. *Anal. Chem*. 2016;88:7946–7958. [[PMC free article](#)] [[PubMed](#)] [[Google Scholar](#)]
56. Lai Z, et al. Identifying metabolites by integrating metabolome databases with mass spectrometry cheminformatics. *Nat. Methods*. 2018;15:53–56. [[PMC free article](#)] [[PubMed](#)] [[Google Scholar](#)]

---

Articles from Scientific Reports are provided here courtesy of **Nature Publishing Group**